An alternative explanation for the density depletions observed by Freja and Viking satellites

K. H. Shah, M. N. S. Qureshi, W. Masood, and H. A. Shah

Citation: AIP Advances **8**, 085010 (2018); doi: 10.1063/1.5040944
View online: https://doi.org/10.1063/1.5040944
View Table of Contents: http://aip.scitation.org/toc/adv/8/8
Published by the American Institute of Physics

An alternative explanation for the density depletions observed by Freja and Viking satellites

K. H. Shah,[1] M. N. S. Qureshi,[2,a] W. Masood,[3,4,5] and H. A. Shah[1,2]
[1]*Department of Physics, FC College (A Chartered University), Lahore 54600, Pakistan*
[2]*Department of Physics, GC University, Lahore 54000, Pakistan*
[3]*The Abdus Salam International Centre for Theoretical Physics, Strada Costiera 11, 34151 Trieste, Italy*
[4]*COMSATS University Islamabad, Islamabad Campus, Park Road, Chak Shahzad, Islamabad 44000, Pakistan*
[5]*National Centre for Physics (NCP) Shahdra Valley Road, P.O. Box 2141, Islamabad 44000, Pakistan*

(Received 22 May 2018; accepted 1 August 2018; published online 9 August 2018)

In this paper, we have studied the linear and nonlinear propagation of ion acoustic waves in the presence of electrons that follow the generalized (r,q) distribution. It has been shown that for positive values of r, which correspond to a flat-topped electron velocity distribution, the nonlinear ion acoustic waves admit rarefactive solitary structures or density depletions. It has been shown that the generalized (r,q) distribution function provides another way to explicate the density depletions observed by Freja and Viking satellites previously explained by proposing Cairns distribution function. https://doi.org/10.1063/1.5040944

I. INTRODUCTION

Ion acoustic waves are one of the fundamental wave modes in a plasma. They compress the density but leave the magnetic field unchanged. The linear theory explains many wave phenomena occurring in nature successfully, however, in many instances it is not adequate and one, therefore, must resort to nonlinear study of waves which bears new and profound results and usually occur over long spatial and temporal scale lengths. Soliton represents nonlinear disturbance in the medium that evinces a spectacular trait: after a collision, the emerging solitons retain their shape. The importance of the concept of solitons has been realized in many fields ranging from fluid dynamics to solid-state physics.[1,2] The nerve impulse[3] and the Great Red Spot on Jupiter[4] have been conjectured to be solitons. Ion acoustic solitons were initially observed experimentally using a double-plasma device. They have also been surmised to be present in the Earth's plasma pause.[5,6]

The data from the satellites has enabled us to construct distribution functions and the remarkable fact that has popped out of this exercise is that the distributions of certain regions of space plasmas show a significant departure from the classical Maxwellian distribution owing to the presence of high-energy tails and/or flat tops.[7–10] Until recently, many problems confronting us in many regions of space were solved using the Maxwellian velocity distribution. However, the data from satellites have shown time and again that the particle distributions in different regions of space exhibit a significant departure from Maxwellian distributions.[11–17] These deviations imply that Maxwellian distribution function in many instances is not sufficient to understand or predict different waves and instabilities. Qureshi et al.[18] in their pioneering work, about a decade ago, gave a new generalized non-Maxwellian electron distribution to incorporate the observed flat-topped behavior at lower energies and modified tails at higher energies in space plasmas. It is emphasized here that (r,q) distribution popped up as

[a]Corresponding Author Dr. M. N. S. Qureshi Department of Physics, GC University, Lahore. E-mail: nouman_sarwar25@hotmail.com

the most general distribution function since it models the distributions generally observed in space plasmas ranging from flat-topped to kappa distributions in the limiting cases.

It was shown that by Dovner et al. that Freja observations of rarefactive solitary or density-depletion structures were related to electric fields that were electrostatic in nature.[19] These structures were also reported by Viking satellite.[20,21] The density-depletion structures which were observed by Freja and Viking satellites can be divided in two categories. The first kind of density depletion structures observed by Freja satellite were associated with the lower-hybrid waves[22] and were reported in the auroral zone by Vago et al.[23] The second kind of density-depletion structures were found to have no association with lower-hybrid waves.[21] To interpret such structures, Cairns et al.[24] presented a new distribution function that successfully generated rarefactive solitary structures in conformity with the observed structures by Freja and Viking satellites.

The main premise of this paper is that observations of density-depletion structures associated with the electrostatic structures observed by various satellites can be explained by employing the generalized (r,q) distribution (double spectral index) for electrons. It happens for those values of index r that are commensurate with distributions that exhibit flatness at low energies. The paper is organized as follows: In Section II, we first introduce double spectral index distribution and explain how the shape of the distribution function depends on the two spectral indices r and q. We then present the governing equations for nonlinear ion acoustic waves consisting of electrons that adhere to the double spectral index (r,q) distribution. In Section III, we delineate the procedure to obtain nonlinear Korteweg de Vries (KdV) equation for our model. We show in detail how the double spectral index distribution affects the linear and nonlinear propagation of sound waves on the ion time scale in plasma. Finally, we recapitulate the important results of this investigation in Section IV.

II. MODEL FORMALISM

Space plasmas often exhibit nonthermal features such as the presence of suprathermal tails[7] and flat tops at low energies.[16,18,25] These nonthermal distributions significantly deviate from the classical Maxwellian distribution function and have successfully been employed to investigate different kinds of phenomena in realistic environments.[13,14,16,17,26–28] In this paper, we use generalized (r,q) distribution function to study the nonlinear ion-acoustic waves which has the following standard three-dimensional form[18]

$$f_{rq}(v) = \frac{3\Gamma[q](q-1)^{-3/(2+2r)}}{4\pi c^{3/2}(2T_e/m_e)^{3/2}\Gamma\left[q-\frac{3}{2+2r}\right]\Gamma\left[1+\frac{3}{2+2r}\right]}\left[1+\frac{1}{q-1}\left(\frac{v^2-2e\phi/m_e}{c(2T_e/m_e)}\right)^{r+1}\right]^{-q} \tag{1}$$

where

$$C = \frac{3(q-1)^{-1/(1+r)}\Gamma\left[q-\frac{3}{2+2r}\right]\Gamma\left[\frac{3}{2+2r}\right]}{2\Gamma\left[q-\frac{5}{2+2r}\right]\Gamma\left[\frac{5}{2+2r}\right]} \tag{2}$$

ϕ is the electrostatic potential, Γ is the gamma function, T_e and m_e are the electron temperature and mass respectively, $(2T_e/m_e)^{1/2}$ is the electron thermal velocity, flatness at lower energies and tail at higher energies are controlled by indices r and q respectively which must hold the conditions $q > 1$ and $q(r+1) > 5/2$. In the limits $r = 0$ and $q \to \infty$ and $r = 0$ and $q \to (\kappa + 1)$, the generalized (r,q) distribution function given in ((Eq. (1)) reduces to the Maxwellian and generalized Lorentzian distributions respectively. To facilitate the visualization of the distribution in velocity space, Fig. 1 shows the plot of generalized (r,q) distribution function (normalized by thermal velocity) for different values of positive r (upper panel) and for different values of negative r (lower panel); limiting cases for kappa (dashed line) and Maxwellian (dotted line) are also given. Enhancement in the flat top or shoulders with the increase of positive r and spiky behavior of the distribution with negative values of r are evident in Fig. 1.

Integrating the (r,q) distribution function (i.e. Eq. (1)) over velocity space, we obtain the total electron number density given by

$$n_e = n_{e0}\left(1 + a_1\varphi + a_2\varphi^2\right) \tag{3}$$

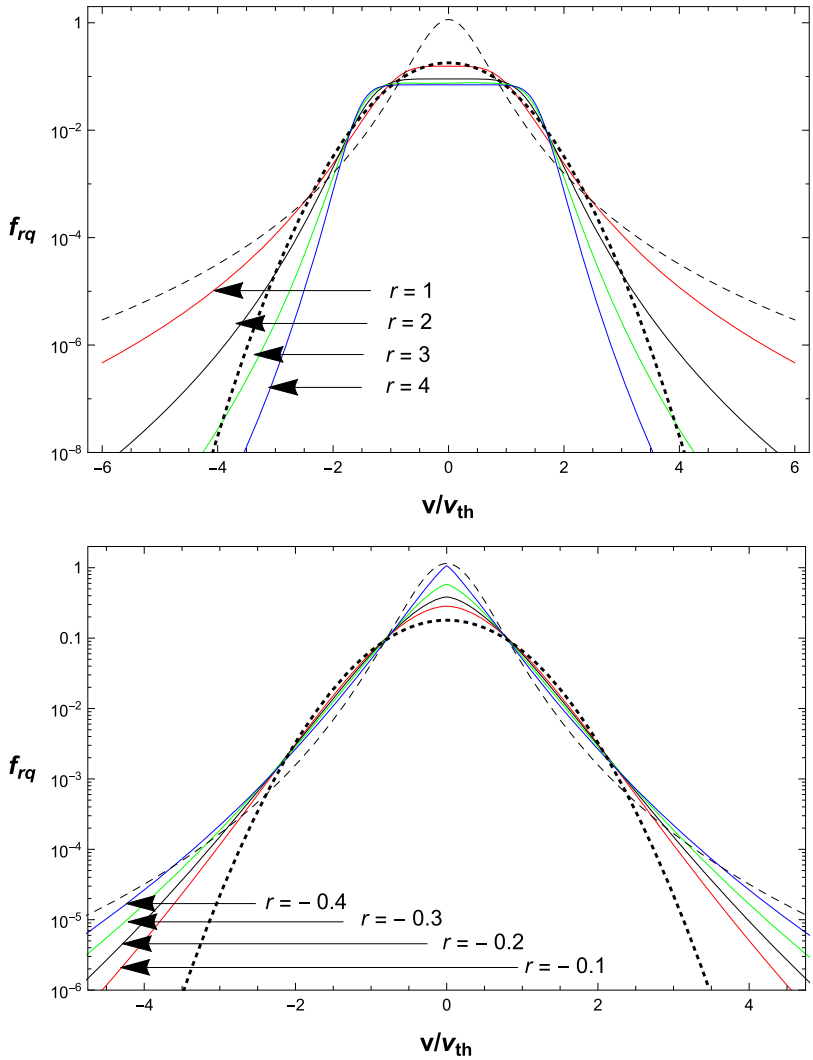

FIG. 1. Generalized (r,q) distribution function for different positive values of $r = 1$ (red), 2 (black), 3 (green), 4 (blue) when $q = 2$ (upper panel), and for different negative values of $r = -0.1$ (red), -0.2 (black), -0.3 (green), -0.4 (blue) when $q = 10$ (lower panel). Limiting cases of kappa distribution (dashed line) and Maxwellian distribution (dotted lines) are also shown.

where $\varphi = e\phi/T_e$, and

$$a_1 = \frac{(q-1)^{-1/(1+r)}\Gamma\left[q - \frac{1}{2+2r}\right]\Gamma\left[\frac{1}{2+2r}\right]}{2c\Gamma\left[q - \frac{3}{2+2r}\right]\Gamma\left[\frac{3}{2+2r}\right]} \tag{4}$$

$$a_2 = -\frac{(1+4r)(q-1)^{-2/(1+r)}\Gamma\left[q + \frac{1}{2+2r}\right]\Gamma\left[\frac{-1}{2+2r}\right]}{8c^2\Gamma\left[q - \frac{3}{2+2r}\right]\Gamma\left[\frac{3}{2+2r}\right]} \tag{5}$$

In the limit $r = 0$ and $q \to \infty$, the constants in Eqs. (4) and (5) become $a_1 = 1$ and $a_2 = 1/2$ and when $r = 0$ and $q \to (\kappa + 1)$, we get $a_1 = \frac{\kappa-1/2}{\kappa-3/2}$ and $a_2 = \frac{(\kappa-1/2)(\kappa+1/2)}{2(\kappa-3/2)^2}$.[15]

The model equations that describe the propagation of ion acoustic waves in one dimension are given here as under:

$$\frac{\partial n}{\partial t} + \frac{\partial (nv)}{\partial x} = 0 \tag{6}$$

$$\frac{\partial v}{\partial t} + v\frac{\partial v}{\partial x} = -\frac{\partial \varphi}{\partial x} \tag{7}$$

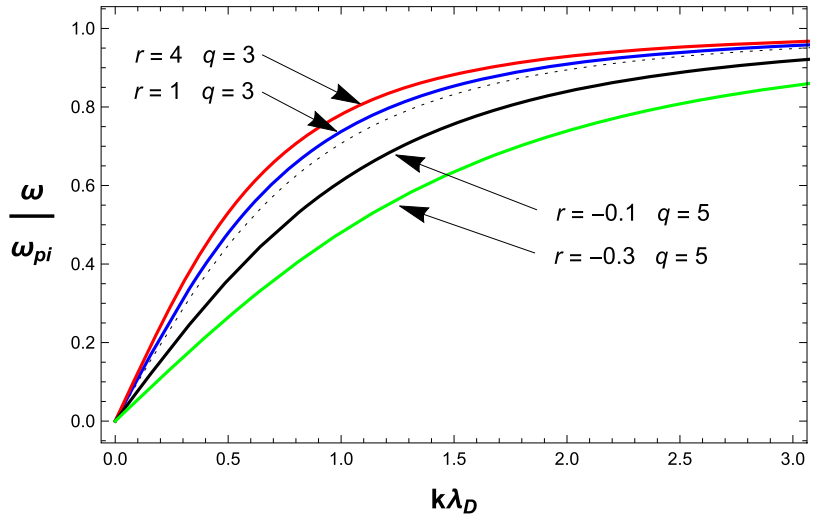

FIG. 2. Linear dispersion relation for ion-acoustic when $r = 0$ and $q \to \infty$ (dotted), $r = 4$, $q = 3$ (red), $r = 1$, $q = 3$ (blue), $r = -0.1$, $q = 5$ (black), $r = -0.3$, $q = 5$ (green).

$$\frac{\partial^2 \varphi}{\partial x^2} = n_e - n \tag{8}$$

In the above equations, n,t,x and v are normalized by n_0, ω_{pi}^{-1}, λ_{Di} and c_s respectively, where $\omega_{pi}^2 = \frac{n_{i0}e^2}{\varepsilon_0 m_i}$, $\lambda_{Di}^2 = \frac{\varepsilon_0 k_B T_e}{n_{i0}e^2}$ and $c_s = \sqrt{\frac{k_B T_e}{m_i}}$. The linear dispersion relation for ion-acoustic waves in (r,q) distributed plasma is

$$\omega^2 = \frac{k^2 c_s^2}{a_1 + k^2 \lambda_D^2} \tag{9}$$

Fig. 2 depicts the linear dispersion relation for specifically chosen values of (r,q) which essentially correspond to different shapes of the distribution function as shown in Figure 1. The limiting Maxwellian form when $r = 0$ and $q \to \infty$ is shown as dotted line. We can see that real frequency is higher than Maxwellian for $r > 0$ whereas it is lower than Maxwellian for $r < 0$.

III. NONLINEAR FORMALISM AND STRUCTURE

We introduce the following stretched coordinates to derive the nonlinear KdV equation,[29]

$$\xi = \varepsilon^{1/2}(x - \lambda t) \quad \text{and} \quad \tau = \varepsilon^{3/2} t \tag{10}$$

where $\varepsilon \ll 1$ and λ is the normalized phase velocity. Making use of the small amplitude approximation method,[29] the quantities n, v and φ are expanded in the following manner:

$$n = 1 + \varepsilon n_1 + \varepsilon^2 n_2 + \ldots \tag{11}$$

$$v = \varepsilon v_1 + \varepsilon^2 v_2 + \ldots \tag{12}$$

$$\varphi = \varepsilon \varphi_1 + \varepsilon^2 \varphi_2 + \ldots \tag{13}$$

Using the stretched variables (i.e., Eq. (10)) and putting the above perturbed quantities in Eqs. (6)–(8), the lowest order in 'ε' gives

$$v_1 = \lambda n_1 \tag{14}$$

$$\lambda v_1 = \varphi_1 \tag{15}$$

$$\lambda^2 = \frac{1}{a_1} \tag{16}$$

The next higher order in ε yields the equations given here as under

$$\frac{\partial n_1}{\partial \tau} - \lambda \frac{\partial n_2}{\partial \xi} + \frac{\partial v_2}{\partial \xi} + \frac{\partial (n_1 v_1)}{\partial \xi} = 0 \tag{17}$$

$$\frac{\partial v_1}{\partial \tau} - \lambda \frac{\partial v_2}{\partial \xi} + v_1 \frac{\partial v_1}{\partial \xi} + \frac{\partial \varphi_2}{\partial \xi} = 0 \tag{18}$$

$$\frac{\partial^2 \varphi_1}{\partial x^2} = -n_2 + a_1 \varphi_2 + a_2 {\varphi_1}^2 \tag{19}$$

The algebraic manipulation of coupled nonlinear partial differential equations (PDE's) given by equations (17)–(19) yield the following KdV equation

$$\frac{\partial \varphi_1}{\partial \tau} + A \frac{\partial {\varphi_1}^2}{\partial \xi} + B \frac{\partial^3 \varphi}{\partial \xi^3} = 0 \tag{20}$$

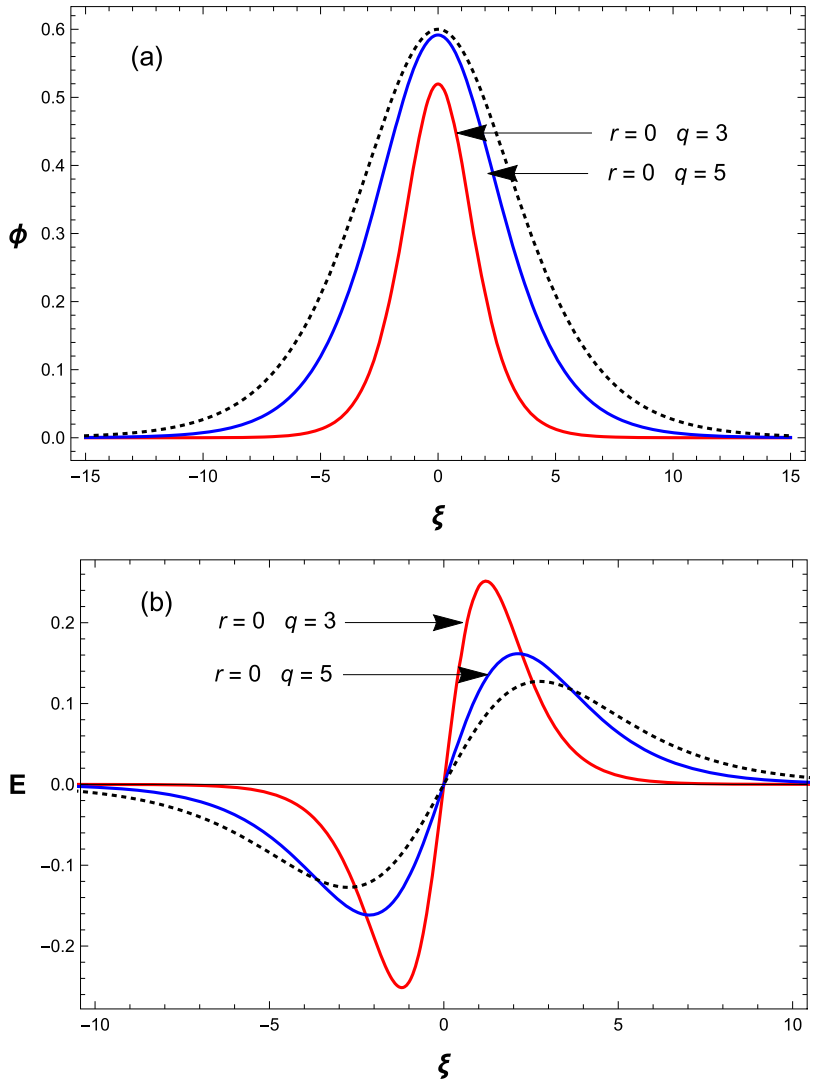

FIG. 3. KdV ion-acoustic hump solitons (a) and corresponding bipolar structures (b) for Maxwellian distribution function when $r = 0$ and $q \to \infty$ (dotted), and kappa distribution when $r = 0$ and $q = 3$ (red), 5 (blue). Here the propagation velocity $u = 0.1$.

where $A = \frac{1}{2}\left(\frac{3}{2\lambda} - \lambda^3 a_2\right)$ and $B = \frac{\lambda^3}{2}$. The solution of Eq. (20) reads as

$$\varphi = \frac{3u}{A}\text{Sech}\left[\frac{\xi}{\Delta}\right]^2 \tag{21}$$

Here the width 'Δ' is given as

$$\Delta = \sqrt{\frac{4B}{u}} \tag{22}$$

Fig. 3(a) shows the soliton solution of KdV equation for limiting cases of (r,q) distribution function, namely, kappa and Maxwellian distributions. In both cases, we obtain hump or compressive solitary structures. It is observed that increasing the spectral index q enhances the amplitude and width of the ion acoustic solitary structures. It can also be seen that in the distributions with modified tails (corresponding to lower q values), the solitary structures form on a shorter spatial scale by comparison with their Maxwellian counterparts (shown with dotted line). Fig. 3(b) shows the bipolar electric field solitary (EFS) structures $E(=-\nabla\varphi)$ corresponding to the compressive solitary structures

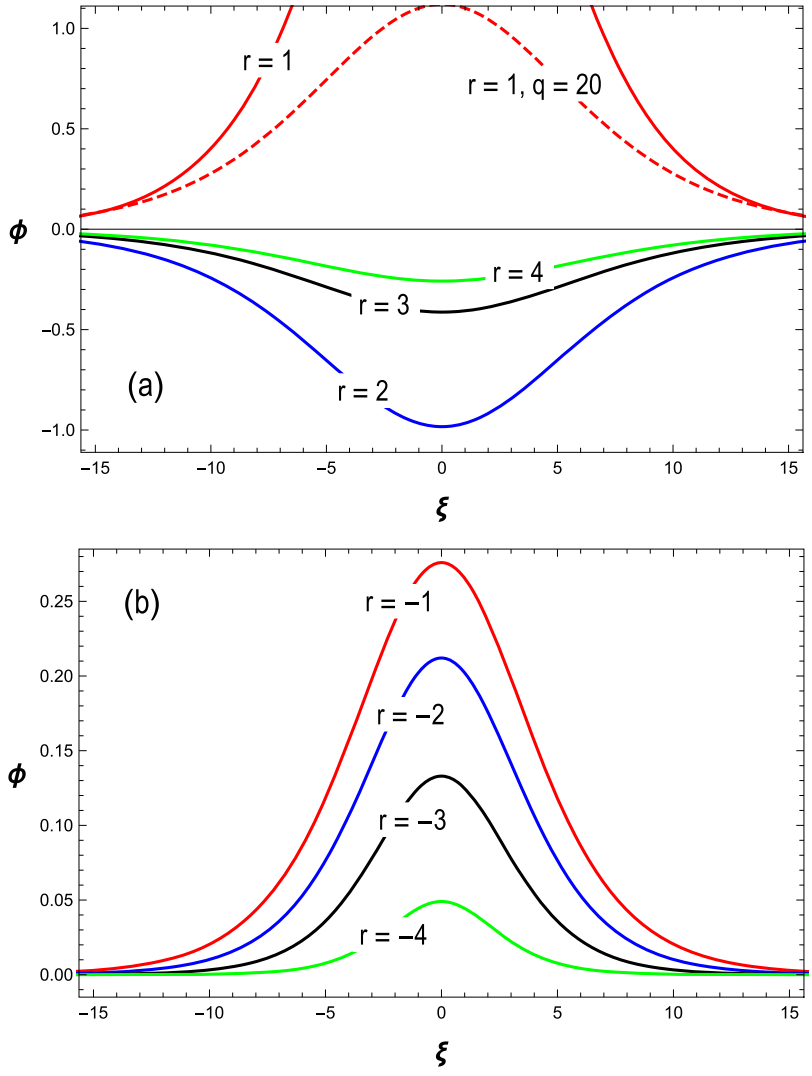

FIG. 4. KdV ion-acoustic solitons for different positive values of r = 1 (red), 2 (blue), 3 (black), 4 (green) when q = 2 and r = 1, q = 20 (red dashed) (a), and for different negative values of r = −0.1 (red), −0.2 (blue), −0.3 (black), −0.4 (green) when q = 10 (b). Here the propagation velocity u = 0.055.

in Fig. 3(a). Bipolar structures are solitary electric field structures often observed in the satellite data with both positive and negative polarities and are responsible for accelerating local plasmas. In Fig. 3(b), note that maximum amplitude and smallest spatial scale of electric field is obtained for that kappa distribution which contains the highest percentage of the nonthermal particles (lowest q value).

Fig. 4(a) shows the propagation characteristics of nonlinear ion acoustic solitary structures for different values of r when $q = 2$ except for the dashed line for which $r = 1$ and $q = 20$. We note that for $r = 1$, flat top in the (r,q) distribution shows close resemblance with the Maxwellian peak (Fig. 1 (upper panel)), and we obtain hump solitons irrespective of the value of q like the Maxwellian case (Fig. 3). For $r \geq 2$, there is switching of the soliton polarity and we obtain dip solitons for which amplitude decreases as r increases. In Fig. 4, we observe that switching depends on the flat-topped nature of the distribution function. As long as the distribution function exhibits flat tops or shoulders, we obtain dip solitons in contrast to the hump solitons which are obtained for the Maxwellian distribution in which there are no flat tops.

In Fig. 5(a), KdV ion-acoustic dip solitons are plotted for different values of r when $q \to \infty$ for (r, q) distribution. Interestingly for $r > 0$, that corresponds to flat top distribution, we obtain

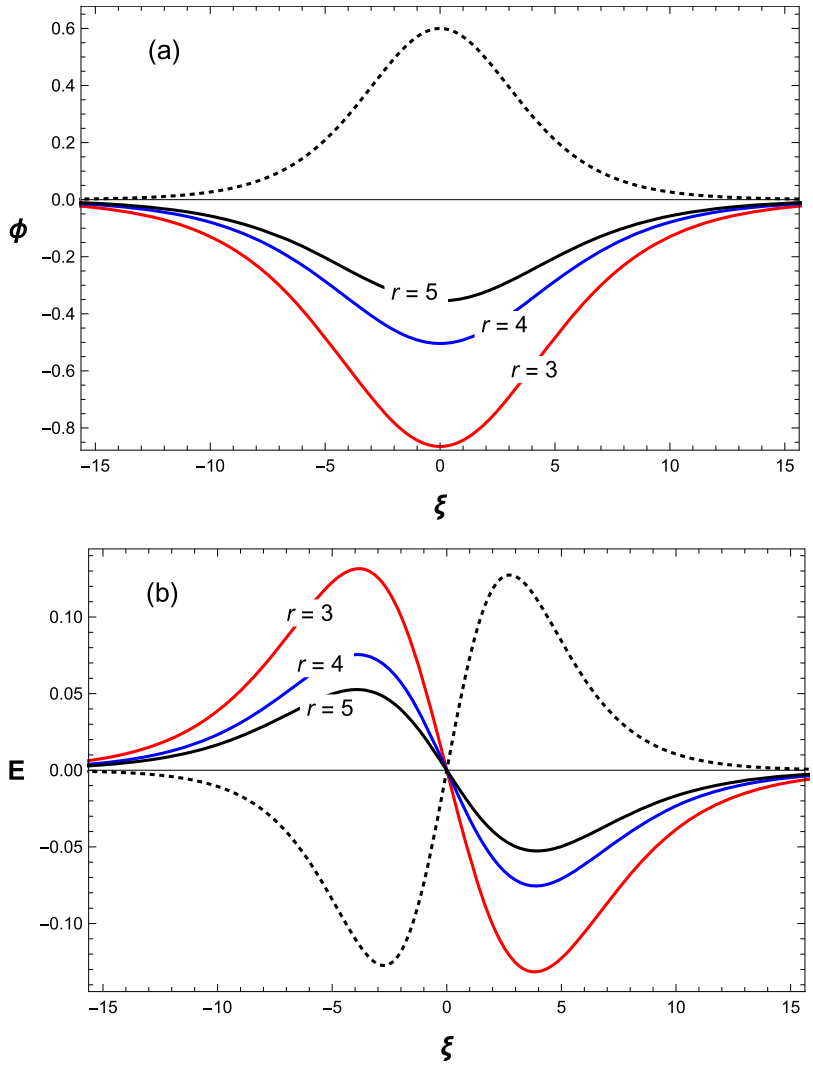

FIG. 5. KdV ion-acoustic dip solitons (a) and corresponding bipolar structures (b) for different values of $r = 3$ (red), 4 (blue), 5 (black) when $q = 2$, Maxwellian case is shown as dotted line. Here the propagation velocity $u = 0.1$.

rarefactive solitons instead of compressive solitons. The amplitude of the soliton mitigates as the flatness parameter or the value of r increases. It is worth mentioning here that flat top distributions are frequently observed in the terrestrial magnetosheath. Cluster satellite has also observed such flat top distributions downstream of the terrestrial bow shock.[13,14,16] They have also been detected in the geomagnetic tail by the ARTEMIS spacecraft.[30] Flat top electron distributions have also been reported around the magnetic reconnection region[31] and in the ramp of the Venus bow shock.[32] It has been earlier pointed out that the Freja observations of density-depletion structures associated with electric fields were surmised to be electrostatic in nature and a new distribution, later termed as Cairns distribution, successfully explained the observations. We have shown here that for flat top distribution functions, that correspond to the positive values of the spectral index r, ion acoustic waves admit rarefactive solitary structures and therefore this is an alternative way to explicate the observed cavitons by Freja and Viking satellites. Fig. 5(b) shows the bipolar EFS structures corresponding to compressive solitons in Fig. 5(a). Note that the maximum amplitude of bipolar EFS structures is obtained for smaller value of r which corresponds to the less flatness.

Fig. 6(a) also shows the KdV ion-acoustic dip solitons but for different values of q keeping the spectral index r as fixed. Once again, we see that the flat top distributions admit rarefactive ion

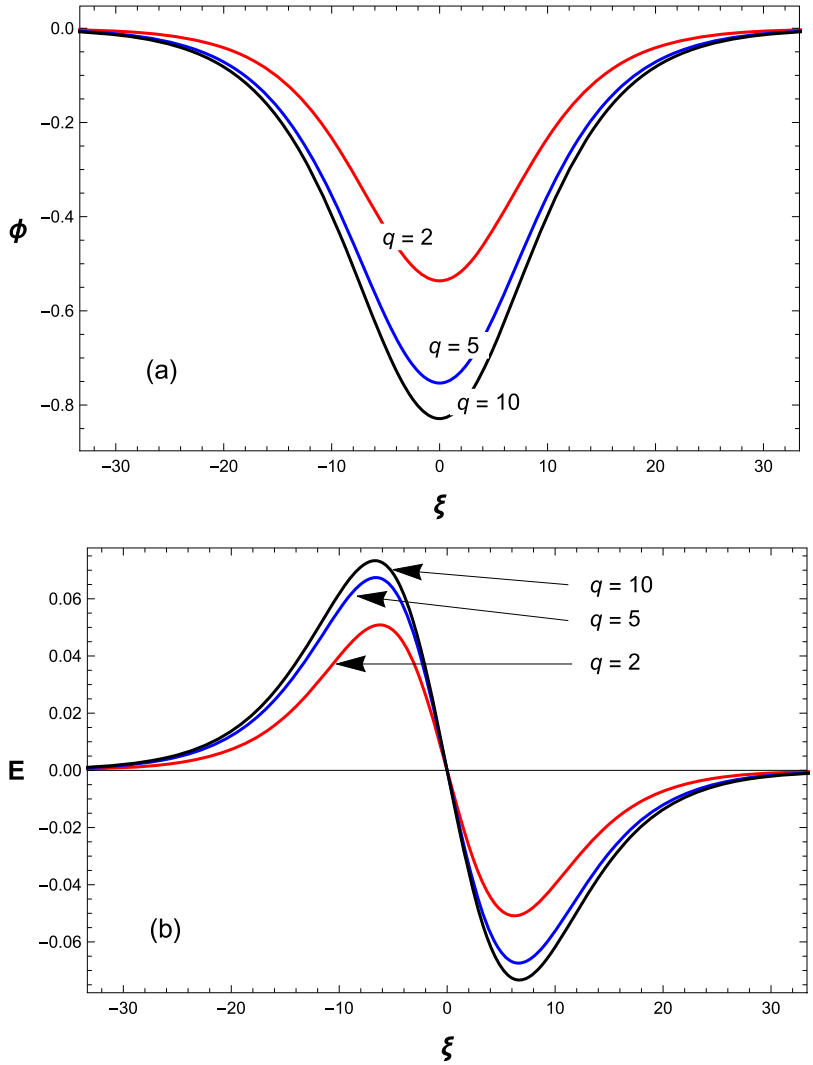

FIG. 6. KdV ion-acoustic dip solitons (a) and corresponding bipolar structures (b) for different values of $q = 2$ (red), 5 (blue), 10 (black) when $r = 2$. Here the propagation velocity $u = 0.1$.

acoustic solitary structures. Here we have explored the effect of modified tail on the nonlinear solitary structure. The amplitude of the rarefactive ion acoustic solitary structures increase with increasing q. Fig. 6(b) depicts the bipolar EFS structures corresponding to the rarefied solitary structures in Fig. 6(a). We can see that amplitude of bipolar EFS structures increases as q increases.

Finally, we explore the effect of negative values of r on the propagation characteristics of the ion acoustic solitary structures in Fig. 7. Before we discuss the results, it is pertinent to mention here that the negative values of r correspond to spiky velocity distribution function as can be seen in Fig. 1. Note that like $r = 0$ case, compressive solitary structures can also be obtained for the negative values of r. Fig. 7(a) manifests that the enhancement in values of negative r attenuates the amplitude and width of the solitary structures. Bipolar EFS structures corresponding to the compressive solitary structures in Fig. 7(a) are plotted in Fig. 7(b). We find that the amplitude as well as spatial scale of bipolar EFS structures decrease as negative value of r increases.

Figs. 8 and 9 depict the maximum amplitude of the density hump and dip solitary structures as a function of the propagation velocity. The span of velocity of the nonlinear structure for spectral indices r and q for a physically acceptable soliton can be seen in Figs. 8 and 9. Note that since we

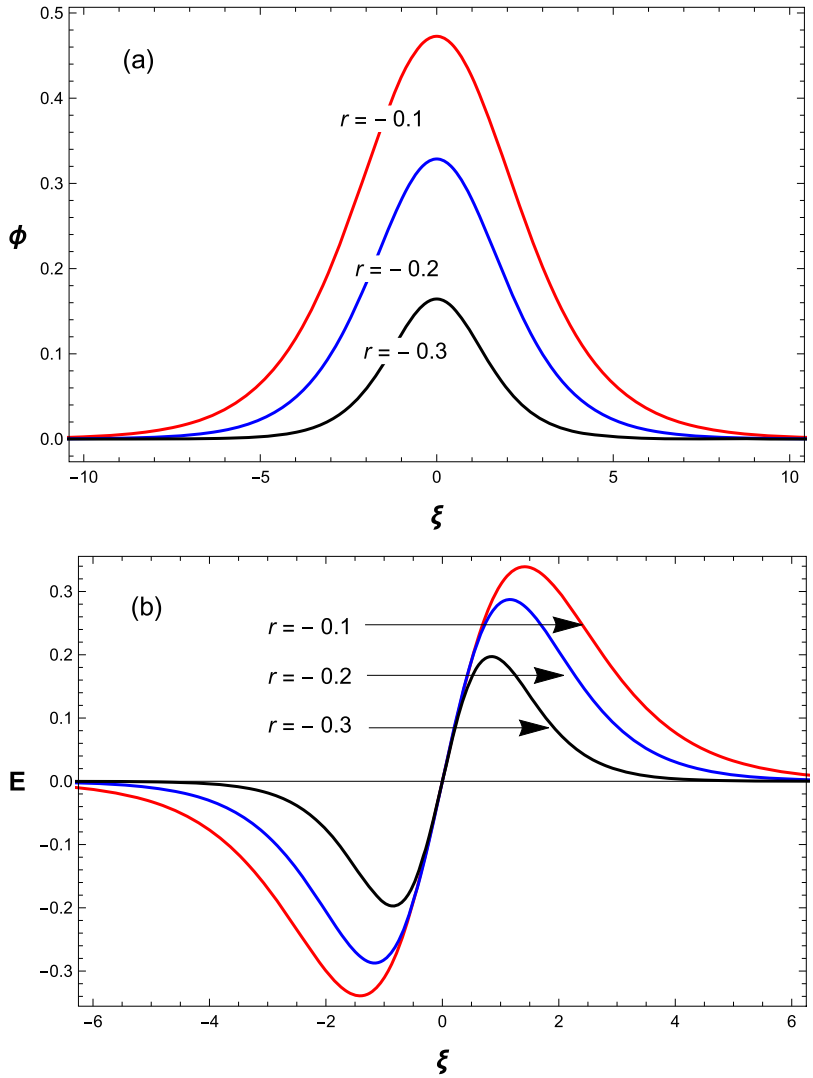

FIG. 7. KdV ion-acoustic hump solitons (a) and corresponding bipolar structures (b) for different values of negative $r = -0.1$ (red), -0.2 (blue), -0.3 (black) when $q = 5$. Here the propagation velocity $u = 0.1$.

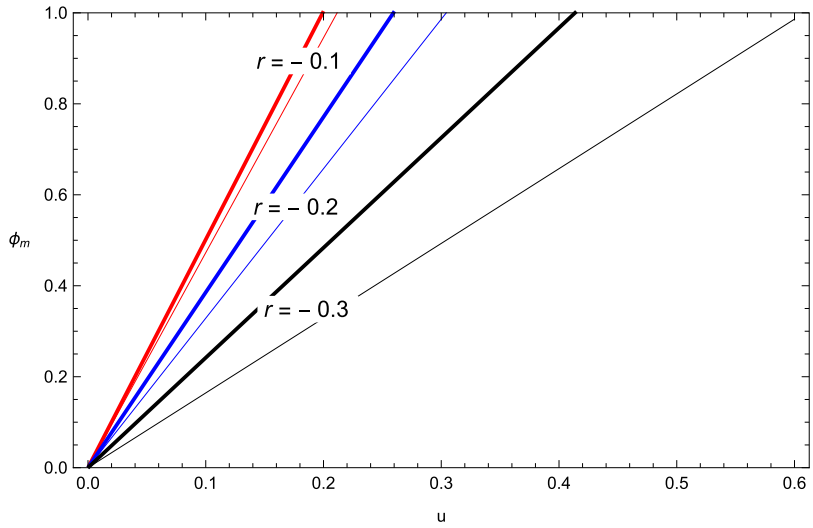

FIG. 8. Maximum amplitude of ion-acoustic hump solitons against the propagation velocity u for different values of negative $r = -0.1$ (red), -0.2 (blue), -0.3 (black) when $q = 5$ (thin), 10 (bold).

are doing a weak turbulent theory therefore the amplitude of the soliton can never exceed unity and therefore a physically acceptable soliton means a soliton whose amplitude remains below unity.

Bipolar EFS structures have been observed by various satellites from different regions of space plasmas such as auroral zone, magnetopause, bow shock, etc. In auroral zone, bipolar EFS structures have been observed by various satellites at different altitudes with amplitudes in the range from 5 – 200 mV/m.[33–37] Such structures have also been observed in the magnetopause with amplitudes up to 25 mV/m[37] and at bow shock with 35 mV/m.[38] Typical values of electron temperature in auroral zone lies in the range $T_e = 6-200$ eV, $T_e \sim 200$ eV around magnetopause and $T_e < 100$ eV around bow shock.[16,39,40] If we consider our model results (Figs. 3–7) and the observed electron temperatures, then the amplitude of bipolar EFS structures lies in the range 1 – 200 mV/m in the auroral zone, 20 – 200 mV/m at the magnetopause and 10 – 100 mV/m at the bow shock, which shows that theoretically predicted values can interpret the observations of bipolar EFS structures from different regions of space plasmas.

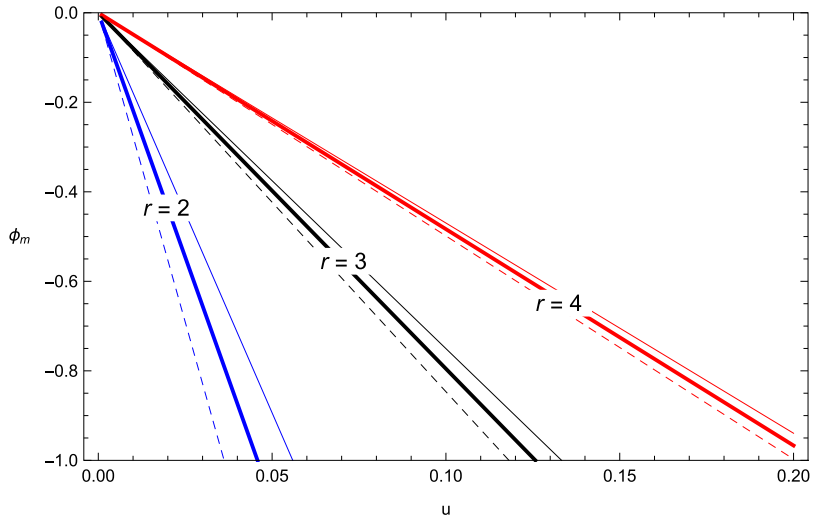

FIG. 9. Maximum amplitude of ion-acoustic dip solitons against the propagation velocity u for different values of $r = 2$ (blue), 3 (black), 4 (red) when $q = 2$ (thin), 3 (bold), 10 (dashed).

IV. CONCLUSION

In this paper, we have investigated nonlinear ion acoustic waves having electrons that adhere to generalized (r,q) distribution. It has been shown in the past that ion acoustic waves with Boltzmannian and kappa distributed electrons allow the formation of only compressive solitary structures. It has been shown in this paper that when electrons are modeled by (r,q) distribution, the nonlinear ion acoustic waves admit both humps and dips in the perturbed potential. It has been observed that for negative values of r and for $r = 0$, the nonlinear ion acoustic waves admit compressive structures; however, for positive values of r which imply flat top distribution (except for $r = 1$), we obtain rarefactive solitary structures or density-depletion structures up to the order of 60 % in agreement with the observations of Freja and Viking satellites. It has been found that the parameter q, which is responsible for altering the tail of the distribution function, alters the spatial scale over which the solitary structures are formed whereas the flatness parameter r is responsible for the change of polarity of the solitary structures. The present paper presents an alternative explanation for the observation of density-depletion structures observed by Freja and Viking satellites based on the observed flat-topped distribution that were earlier explained by Cairns et al.[24] using Cairns distribution which is yet to be observed. The bipolar EFS structures observed in space plasmas have also been discussed to fortify our explanation.

ACKNOWLEDGMENTS

Authors K. H. Shah, M. N. S. Qureshi and H. A. Shah acknowledge the Higher Education Commission (HEC) grant no. 20-2595/NRPU/R&D/HEC/13. The author M. N. S. Qureshi acknowledges the GC University, Lahore grant no. 101/ORIC/17.

[1] K. Lonngren and A. Scott, Eds., *Solitons in Action*, New York, Academic Press, Inc., (1978).
[2] C. Rebbi, Sci. Amer. **240**, 76 (1979).
[3] H. C. Tuckwell, Science **205**, 493 (1979).
[4] T. Maxworthy and L. G. Redekopp, Icarus **29**, 261 (1976).
[5] H. Kikuchi, J. Atmos. Terr. Phys. **38**, 1055 (1976).
[6] H. Ikezi, R. Taylor, and D. Baker, Phys. Rev. Lett. **25**, 11 (1970).
[7] D. Summers and R. M. Thorne, Phys. Fluids B **3**, 1835 (1991).
[8] D. Summers and R. M. Thorne, J. Geophys. Res. **97**, 16827, https://doi.org/10.1029/92ja01664 (1992).
[9] S. Xue, R. M. Thorne, and D. Summers, J. Geophys. Res. **98**, 17475, https://doi.org/10.1029/93ja00790 (1993).
[10] D. Summers, R. M. Thorne, and H. Matsumoto, Phys. Plasmas **3**, 2496 (1996).
[11] S. J. Schwartz, J. Geophys. Res. **93**, 12923, https://doi.org/10.1029/ja093ia11p12923 (1988).
[12] M. R. Collier, D. C. Hamilton, G. Gloeckler, P. Bochsler, and R. B. Sheldon, Geophys. Res. Lett. **23**, 1191, https://doi.org/10.1029/96gl00621 (1996).
[13] W. Masood, S. J. Schwartz, M. Maksimovic, and A. N. Fazakerley, Ann. Geophysicae **24**, 1725 (2006).
[14] W. Masood and S. J. Schwartz, J. of Geophys. Res. **113**, A01216, https://doi.org/10.1029/2007ja012715 (2008).
[15] W. Masood, M. N. S. Qureshi, P. H. Yoon, and H. A. Shah, J. Geophys. Res. **120**, 101, https://doi.org/10.1002/2014ja020459 (2015).
[16] M. N. S. Qureshi, W. Nasir, W. Masood, P. H. Yoon, H. A. Shah, and S. J. Schwartz, J. Geophys. Res. **119**, 10059, https://doi.org/10.1002/2014ja020476 (2014).
[17] T. Aziz, W. Masood, M. N. S. Qureshi, H. A. Shah, and P. H. Yoon, Phys. Plasmas **23**, 062307 (2016).
[18] M. N. S. Qureshi, H. A. Shah, G. Murtaza, S. J. Schwartz, and F. Mahmood, Physics of Plasmas **11**, 3819 (2004).
[19] P. O. Dovner, A. I. Eriksson, R. Bostrom, and B. Holback, Geophys Res. Lett. **21**, 1827, https://doi.org/10.1029/94gl00886 (1994).
[20] R. Bostrom, G. Gustafsson, B. Holback, G. Holmgren, H. Koskinen, and P. Kintner, Phys. Rev. Lett. **61**, 82 (1988).
[21] R. Bostrom, IEEE Trans. Plasma Sci. **20**, 756 (1992).
[22] A. I. Eriksson, B. Holback, P. O. Dovner, R. Boström, G. Holmgren, M. Andrd, L. Eliasson, and P. M. Kinruer, Geophys. Res. Lett. **21**, 1843, https://doi.org/10.1029/94gl00174 (1994).
[23] J. L. Vago, P. M. Kintner, S. W. Chesney, R. L. Arnoldy, K. A. Lynch, T. E. Moore, and C. J. Pollock, J. Geophys. Res. **97**, 16935, https://doi.org/10.1029/92ja01526 (1992).
[24] R. A. Cairns, A. A. Mamun, R. Bingham, R. Boström, R. O. Dendy, C. M. C. Nairn, and P. K. Shukla, Geophys. Res. Lett. **22**, 2709, https://doi.org/10.1029/95gl02781 (1995).
[25] M. N. S. Qureshi, J. K. Shi, and S. Z. Ma, Phys. Plasmas **12**, 122902 (2005).
[26] Z. Kiran, H. A. Shah, M. N. S. Qureshi, and G. Murtaza, Sol. Phys. **236**, 167 (2006).
[27] T. K. Balaku and M. A. Hellberg, Phys. Plasmas **15**, 123705 (2008).
[28] K. H. Shah, M. N. S. Qureshi, W. Masood, and H. A. Shah, Phys. Plasmas **25**, 042303 (2018).
[29] H. Washimi and T. Tanuiti, Phts. Rev. Lett. **17**, 996 (1966).
[30] D. Zhao, S. Fu, G. K. Parks, W. Sun, Q. Zong, D. Pan, and T. Wu, Phys. Plasmas. **24**, 082903 (2017).
[31] Y. Asano, R. Nakamura, I. Shinohara, M. Fujimoto, T. Takada, W. Baumjohann, C. J. Owen, A. N. Fazakerley, A. Runov, T. Nagai, E. A. Lucek, and H. Rème, J. Geophys. Res. **113**, A01207, https://doi.org/10.1029/2007ja012461 (2008).

[32] W. C. Knudsen, D. E. Jones, B. G. Peterson, and C. E. Knadler, Jr., J. Geophys. Res. **121**, 7753, https://doi.org/10.1002/2016ja022526 (2016).
[33] M. Termine, K. Cerny, W. Lotko, and F. S. Mozer, Phys. Rev. Lett. **48**, 17 (1982).
[34] F. S. Mozer, R. Ergun, M. Temerin, C. Cattell, J. Dombeck, and J. Wygant, Phys. Rev. Lett. **79**, 7 (1997).
[35] S. R. Bounds, R. F. Pfaff, S. F. Knowlton, F. S. Mozer, M. A. Temerin, and C. A. Kletzing, J. Geophys. Res. **104**, 28709, https://doi.org/10.1029/1999ja900284 (1999).
[36] J. Dombeck, C. Cattell, J. Crumley, W. K. Peterson, H. L. Collin, and C. Kletzing, J. Geophys. Res. **106**, 19013, https://doi.org/10.1029/2000ja000355 (2001).
[37] C. Cattell, J. Crumley, J. Dombeck, and J. Wygant, Geophys. Res. Lett. **29**, 5, https://doi.org/10.1029/2001gl014046 (2002).
[38] R. Behlke, M. André, S. D. Bale, J. S. Pickett, C. A. Cattell, E. A. Lucek, and A. Balogh, Geophys. Res. Lett. **31**, L16805, https://doi.org/10.1029/2004gl019524 (2004).
[39] R. E. Ergun, L. Andersson, D. S. Main, Y. J. Su, C. W. Carlson, J. P. McFadden, and F. S. Mozer, Phys. Plasmas **9**, 3685 (2002).
[40] R. E. Ergun, L. Andersson, C. W. Carlson, D. L. Newman, and M. V. Goldman, Nonlinear Processes in Geophysics **10**, 45 (2003).